



Research article

Scheduling optimization of electric energy meter distribution vehicles for intelligent batch rotation

Zhaolei He^{a,b}, Xinbo Zhou^c, Cong Lin^{a,b}, Jing Zhao^{a,b}, Hengjie Yu^{a,b}, Rui Fang^{a,b}, Jin Liu^{a,b}, Xin Shen^{a,b}, Nan Pan^{d,*}

^a Metering Center of Yunnan Power Grid Co., Ltd., Kunming, 650011, China

^b Key Laboratory of Electric Power Measurement (China Southern Power Grid), Kunming, 650217, China

^c Faculty of Information Engineering and Automation, Kunming University of Science and Technology, Kunming, 650500, China

^d Faculty of Civil Aviation and Aeronautics, Kunming University of Science and Technology, Kunming, 650500, China

ARTICLE INFO

Keywords:

Electric meter rotation
Multi-level scheduling
Levy flight strategy
Cauchy mutation
Opposition-based learning
Grey wolf optimization

ABSTRACT

As industrial technology continues to advance through integration, society's demand for electricity is rapidly increasing. To meet the requirements of refined grid management and address the elevated challenges arising from the increased electrical load, this paper delves into the investigation of distribution vehicle scheduling for the practical scenario of batch rotation of smart meters. Initially, based on the practical distribution task requirements of a provincial metrology verification center, a multi-level optimization model is constructed for the batch rotation and distribution vehicle scheduling of smart meters. The primary objective is to maximize the enhancement of smart meter distribution efficiency while minimizing the overall distribution cost. Moreover, this paper introduces a refined Grey Wolf Optimization algorithm (OLC-GWO) based on Opposition-based Learning, Levy flight strategy, and Cauchy mutation to solve the model. By generating an opposite population to improve the quality of initial feasible solutions and further harnessing the global search capabilities of Levy flight and Cauchy mutation operators, the algorithm's effectiveness is enhanced. The algorithm is subjected to testing using multiple benchmark functions and its performance is compared with variants of GWO, as well as several cutting-edge intelligent optimization algorithms including Particle Swarm Optimization (PSO), Harris Hawks Optimization (HHO), and Honey Bee Algorithm (HBA). The results indicate that OLC-GWO exhibits excellent performance in terms of convergence speed and optimization capability. Finally, the improved algorithm is subjected to simulation experiments by incorporating order data from the practical distribution operations of a provincial metrology verification center. The outcomes verify the efficiency of the proposed algorithm, reinforcing the practical significance of the established model in addressing the real-world challenge of batch rotation and distribution vehicle scheduling for smart meters.

* Corresponding author.

E-mail address: nanpan@kust.edu.cn (N. Pan).

<https://doi.org/10.1016/j.heliyon.2024.e26516>

Received 8 September 2022; Received in revised form 2 February 2024; Accepted 14 February 2024

Available online 21 February 2024

2405-8440/Â© 2024 The Authors. Published by Elsevier Ltd. This is an open access article under the CC BY-NC-ND license (<http://creativecommons.org/licenses/by-nc-nd/4.0/>).

1. Introduction

1.1. Background

The rise of the smart grid signifies the profound integration of emerging fields such as information technology, communication technology, sensing and detection technology, and energy power technology with the physical infrastructure of the power grid. This convergence creates a power system that is highly informational, automated, refined, and interactive. This modernized power grid possesses exceptional power regulation capabilities, grid structural flexibility, and energy service quality, offering unprecedented opportunities for energy distribution and management [1].

Within the comprehensive construction of the smart grid, the intelligent development of grid logistics scheduling has become a pivotal aspect of achieving optimized operations in the smart grid. Traditional production scheduling methods struggle to address the heightened complexity and challenges faced by new-generation power grid material distribution scheduling, which includes multi-level distribution networks, heterogeneous vehicle types, and constraints related to multiple material types and time windows. Consequently, the problem of batch rotation and distribution vehicle scheduling for electricity meters in the context of the smart grid has emerged as a challenging optimization problem, presenting new requirements for achieving efficient energy distribution.

1.2. Literature review

The core of the smart meter distribution scheduling problem is a multi-objective vehicle routing problem with complex constraints, which has been extensively studied by scholars both domestically and internationally. Since the introduction of the Vehicle Routing Problem (VRP), numerous variants have arisen to address academic research and practical application needs. These include Vehicle Routing Problems with Time Windows (VRPTW) [2], Green Vehicle Routing Problem (GVRP) [3], Multi-Objective Vehicle Routing Problem (MOVRP) [4], and Multi-Objective Vehicle Routing Problem with Flexible Time Windows (MOVRPFlexTW) [5].

In reference [6], a novel variant, the Two-Echelon Vehicle Routing Problem with Time Windows, Intermediate Facilities, and Occasional Drivers (2E-VRPTW-IF-OD), was introduced along with a robust solution. To address the challenge of obtaining consistent Pareto-optimal solutions with minimal amplitude differences for Multi-Objective Vehicle Routing Problem with Time Windows (MOVRPTW), reference [7] proposed a parallelized algorithm based on a two-stage distributed disruption-reconstruction hybrid genetic algorithm. In Ref. [8], a method based on Radial Basis Function Network (RBFN) was suggested to solve the Multi-Objective Vehicle Routing Problem with Stochastic Demands (MO-VRPSD). Considering urban freight contexts and the emergence of “grey zone” customers between city centers and surrounding areas, reference [9] formulated a two-stage multi-objective vehicle dispatch method, offering valuable insights for sustainable urban logistics planning.

In solving vehicle dispatch problems, existing research mainly falls into two categories: exact algorithms and heuristic algorithms. The former is commonly used for small-scale problems, while the latter excels in addressing large-scale and complex issues. Notable exact algorithms encompass branch and bound, linear programming, and dynamic programming methods. In Ref. [10], for the waste sorting transportation problem, a stabilized branch-and-price-and-cut algorithm based on an extended network is proposed. This approach simplifies the pricing subproblem through network extension and enhances convergence performance using stabilization techniques. Although such algorithms yield favorable results for small-scale logistics dispatch, their efficiency drastically diminishes as problem size grows.

Heuristic algorithms include ant colony optimization [5,11], genetic algorithm [12–14], simulated annealing [15], and more. In Ref. [16], a tailored multi-objective hybrid metaheuristic algorithm is designed for the Factory-in-a-box manufacturing vehicle routing problem. This algorithm directly considers the specific attributes of the problem, rendering it well-suited for its modeled scenarios. In Ref. [17], a hybrid enhanced GSA-PSO scheme is proposed, merging gravitational search algorithm and particle swarm optimization (PSO) while introducing adaptive inertia vectors, learning factors, and chaotic initialization. This scheme is applied to optimize load dispatch in microgrids with electric vehicles. In Ref. [18], a novel agent-based metaheuristic architecture is introduced, treating each vehicle as an agent and using centralized agent cooperation for search control.

Given the robustness and parallelism of heuristic algorithms, they exhibit superior optimization capabilities in solving large-scale complex problems. Thus, this study leverages the relatively novel Grey Wolf Optimization (GWO) algorithm for model optimization. Variations and improvements of GWO have emerged for its applications in diverse real-world scenarios. Reference [19] enhances GWO by addressing search agent positioning and boundary handling, particularly for intelligent grid planning. In Ref. [20], a multi-mechanism collaborative improved Grey Wolf Optimization algorithm is proposed. This introduces an evolutionary boundary constraint mechanism for handling individuals crossing boundaries. Gaussian mutation strategy and spiral function are incorporated for perturbation, while an improved sigmoid function acts as a nonlinear convergence factor, enhancing algorithm generality and robustness.

1.3. Research motivation and objectives

While a substantial body of research has focused on VRP and its variants, comprehensive solutions for the smart meter distribution scheduling problem remain limited. Particularly, addressing the complexities of multi-tiered distribution networks, heterogeneous vehicle types, diverse material categories, and time windows in the context of large-scale smart meter rotation poses a challenge, lacking a comprehensive optimization approach.

In this context, this study centers around real-world scenarios of extensive smart meter rotation. It comprehensively addresses

conditions within multi-tiered distribution networks, including constraints such as heterogeneous vehicle types and distribution costs. By incorporating vehicle, time, and transportation costs as optimization objectives, a multi-level optimization model is established for intelligent smart meter batch rotation vehicle scheduling, providing reference for related research. Moreover, considering the weak alignment between existing algorithmic models and the literature, coupled with limited global development capabilities of algorithms and a tendency to prematurely converge to local optima, this paper introduces an improved Grey Wolf Optimization algorithm. This algorithm not only establishes the mapping relationship between the algorithm and the model but also effectively breaks free from local optima, ultimately achieving an optimal distribution strategy for intelligent smart meter batch rotation within the power grid. Through these endeavors, the paper aims to present a novel and practically valuable solution, along with an effective optimization approach, for the intelligent smart meter batch rotation scheduling problem.

2. Multi-stage scheduling model of smart meter batch rotation distribution vehicles

2.1. Nomenclature

Symbol	Description	Unit
Constant		
d_{Si}	The distance between metering center S and power supply bureau i	km
d_{ij}	The distance between power supply bureau i and power supply bureau j	km
d_{im}	The distance between power supply bureau i and power substation m	km
d_{mn}	The distance from power station m to power substation n	km
V_d	The transport speed of model d	km/h
F_d	The fixed cost of a single sortie for model d	CNY
C_d	Unit distance transportation cost of model d	CNY/h
G	Labor cost per unit time of transportation	CNY/h
W_p	Storage cost per unit time of turnover stack	CNY/h
G_{M_p}	The quality of a single meter M_p	kg
C_p	Labor delivery costs to reach a single site	CNY
L_d	Maximum load limit for model d	kg
β_1	Maximum number of containers stored	
β_2	Maximum storage quantity of revolving stack	
$I(m, M_p)$	Consumption of electricity meter M_p by power substation m	
$S(m, M_p)$	Meter M_p inventory of power substation m before replenishment	
$Q(m, M_p)$	Demand for electricity meters M_p in power substation m	
Set		
C_S	Vehicle set of metering center S	
C_i	Vehicle set of power supply bureau i	
E	Set of power supply bureaus	
U	set of meter types	
P_i	Set of power supply substations under the jurisdiction of power supply bureau i	
Variable		
$Q_{(i, M_p)}^{k_S}$	The number of vehicles k_S distributed to the power supply Bureau i meter M_p	
$Q_{(m, M_p)}^{k_i}$	The number of vehicles k_i distributed to the power substation m meter M_p	
0-1 variable		
q_{k_S}	$q_{k_S} = 1$ when vehicle k_S is used and 0 otherwise	
q_{k_i}	$q_{k_i} = 1$ when vehicle k_i is used and 0 otherwise	
$X_{Si}^{k_S}$	$X_{Si}^{k_S} = 1$ when the vehicle k_S goes from the metering center S to the power supply bureau i , and 0 otherwise	
$X_{ij}^{k_S}$	$X_{ij}^{k_S} = 1$ when the vehicle k_S goes from power supply bureau i to power supply bureau j , and 0 otherwise	
$X_{im}^{k_i}$	$X_{im}^{k_i} = 1$ when vehicle k_i goes from power supply bureau i to power substation m , and 0 otherwise	
$X_{mn}^{k_i}$	$X_{mn}^{k_i} = 1$ when the vehicle k_i goes from power substation m to power substation n , and 0 otherwise	

2.2. Problem description

Within a supply cycle T , each substation compiles the demand for smart meters in their responsible transformer area and reports it to the Power Supply Bureau. The Power Supply Bureaus then collectively report to their respective Metering Centers, forming a consolidated demand. This process ultimately facilitates batch smart meter rotation and distribution within the two-tier distribution network " Metering Center - > Power Supply Bureau - > Power Substation."

Fig. 1 shows the overall schematic diagram of intelligent warehouse of Provincial Metering Center. Assume that the provincial metering center S has N power supply Bureau in the responsible area. Denote the power supply bureau as $E = \{1, 2, \dots, i, j, \dots, N\}$. Any power supply bureau i has N_i power substations $P_i = \{1, 2, \dots, m, n, \dots, N_i\}$. For the first-level network, the distribution vehicle set of metering center S is $C_S = \{1, 2, \dots, k_S, \dots, K_S\}$. For the second-level distribution network, the distribution vehicle set of any power supply bureau i is $C_i = \{1, 2, \dots, k_i, \dots, K_i\}$, where the transport vehicle type set is: $\{1, 2, \dots, d, \dots, D\}$. To obtain the optimal scheduling scheme for smart meter batch rotation distribution vehicles, improve the distribution efficiency of smart meters in provincial metering centers, and reduce the overall distribution cost, this paper constructs the following multi-level optimization model for smart meter batch rotation distribution vehicles scheduling.

2.3. Model assumptions

- 1) Vehicles in each distribution network are responsible solely for completing tasks within their respective networks, returning to their originating metering centers or power supply bureaus upon task completion.
- 2) Second-level distribution tasks can commence once first-level network tasks are finished.
- 3) Loading and unloading times of transport vehicles are not considered.
- 4) Cross-docking between transport vehicles is not accounted for.
- 5) Distribution vehicles are subject to payload limits, and outsourced vehicles used should have a volume smaller than the vehicle capacity when fully loaded.

2.4. Model building

Consider splitting the overall two-tier distribution network “Metering Center -> Power Supply Bureau -> Power Substation” into two layers of distribution networks: the first layer is from the Metering Center to the Power Supply Bureau, and the second layer is from the Power Supply Bureau to the Substation. Furthermore, decompose the second-layer distribution network to obtain the distribution relationships between each Power Supply Bureau and Substation. The total cost of a distribution order includes fixed vehicle costs, time costs, and transport distribution costs. Introduce decision variables Q , q , and X as 0–1 variables to determine vehicle usage, the number of distributions, and distribution paths, respectively. Consequently, the various costs can be represented as follows:

1. Fixed cost of vehicle delivery:

The fixed cost of vehicle delivery is the fixed cost of each type of vehicle per unit trip in the two-level distribution network, as shown in Eq. (1).

$$C_f = \sum_{k_s \in C_s} \sum_{i \in E} \sum_{k_i \in C_t} (F_d \cdot q_{k_s} \cdot q_{k_i}). \quad (1)$$

2. Time cost:

The time cost, which includes the broad cost of labor such as driver driving and on-board operation, and the cost of turnover pallet storage per unit of time, is a cost that increases over time, as shown in Eqs (2) and (3).

$$C_{t1} = \sum_{k_s \in C_s} \sum_{i, j \in E} G(X_{Si}^{k_s} d_{Si} / V_d + X_{ij}^{k_s} d_{ij} / V_d) + \sum_{i \in E} \sum_{k_i \in C_t} \sum_{m, n \in P_i} G(X_{im}^{k_i} d_{im} / V_d + X_{mn}^{k_i} d_{mn} / V_d), \quad (2)$$

$$C_{t2} = \sum_{i \in E} \sum_{m \in P_i} \sum_{M_P \in U} W_P \left[\frac{Q(m, M_P) + S(m, M_P) - I(m, M_P)}{\beta_1 \beta_2} \right]. \quad (3)$$

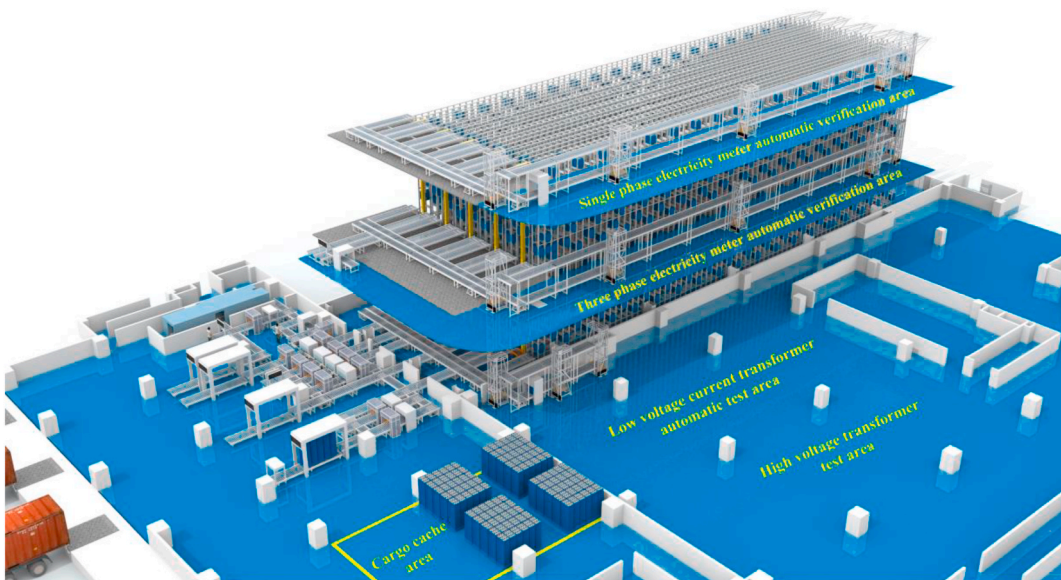


Fig. 1. Provincial metering center intelligent warehouse overall diagram.

3. Transportation and distribution costs:

Considering that the distribution scheme should minimize the transportation and distribution distance and reduce the number of repeated arrivals at each station, the transportation and distribution cost includes the distribution cost per unit distance and the distribution cost required to reach each station, as shown in Eqs (4) and (5).

$$C_{trans1} = \sum_{k_S \in C_S} \sum_{i,j \in E} C_d (X_{Si}^{k_S} d_{Si} + X_{ij}^{k_S} d_{ij}) + \sum_{i \in E} \sum_{k_i \in C_i} \sum_{m,n \in P_i} C_d (X_{im}^{k_i} d_{im} + X_{mn}^{k_i} d_{mn}), \quad (4)$$

$$C_{trans2} = \sum_{k_S \in C_S} \sum_{i,j \in E} C_P (X_{Si}^{k_S} + X_{ij}^{k_S}) + \sum_{i \in E} \sum_{k_i \in C_i} \sum_{m,n \in P_i} C_P (X_{im}^{k_i} + X_{mn}^{k_i}). \quad (5)$$

Thus, the objective function of the multi-level optimization model of distribution vehicle scheduling is shown in Eq. (6).

$$\min Z = C_f + C_{i1} + C_{i2} + C_{trans1} + C_{trans2}. \quad (6)$$

2.5. Constraints analysis

Considering the cargo limitations of each type of delivery vehicle, there are constraints as shown in Eqs. (7) and (8).

$$Q_{(i,M_P)}^{k_S} G_{M_P} \leq L_d (i \in E, k_S \in C_S), \quad (7)$$

$$Q_{(m,M_P)}^{k_i} G_{M_P} \leq L_d (i \in E, m \in P_i, k_i \in C_i). \quad (8)$$

To ensure that each vehicle returns to the metering center or power supply bureau after completing the distribution task, each vehicle must leave after arriving at a station, thus the constraints shown in Eqs. (9)–(12).

$$\sum_{k_S \in C_S} q_{k_S} = \sum_{k_S \in C_S} \sum_{i \in E} X_{iS}^{k_S}, \quad (9)$$

$$\sum_{i \in E} \sum_{k_i \in C_i} \sum_{m \in P_i} X_{im}^{k_i} = \sum_{i \in E} \sum_{k_i \in C_i} \sum_{m \in P_i} X_{ni}^{k_i}, \quad (10)$$

$$\sum_{i \in E} \sum_{k_S \in C_S} X_{ij}^{k_S} = \sum_{j \in E} \sum_{k_S \in C_S} X_{ij}^{k_S}, \quad (11)$$

$$\sum_{i \in E} \sum_{k_i \in C_i} \sum_{m \in P_i} X_{mn}^{k_i} = \sum_{i \in E} \sum_{k_i \in C_i} \sum_{n \in P_i} X_{mn}^{k_i}. \quad (12)$$

To prevent drivers from exerting themselves excessively, each vehicle should have a maximum delivery distance limit, as shown in Eqs (13) and (14).

$$\sum_{i,j \in E} (X_{Si}^{k_S} d_{Si} + X_{ij}^{k_S} d_{ij}) \leq \text{dist}(k_S \in C_S), \quad (13)$$

$$\sum_{m,n \in P_i} (X_{im}^{k_i} d_{im} + X_{mn}^{k_i} d_{mn}) \leq \text{dist}(i \in E, k_i \in C_i). \quad (14)$$

Considering the demand continuity constraints of the power supply bureau and the power substation, Eqs. (15) and (16) are obtained.

$$Q(m, M_P) = \sum_{k_i \in C_i} Q_{(m,M_P)}^{k_i} (m \in P_i), \quad (15)$$

$$Q(i, M_P) = \sum_{k_S \in C_S} Q_{(i,M_P)}^{k_S} (i \in E), \quad (16)$$

To eliminate possible subloops in the two-level network during the scheduling process, assume that $E_{k_S} = \{1, 2, \dots, N_{k_S}\}$ represents the set of power supply bureau responsible for vehicle k_S , and $E_{k_i} = \{1, 2, \dots, N_{k_i}\}$ represents the set of power substations responsible for vehicle k_i , there are constraints shown in Eqs. (17) and (18).

$$\begin{cases} \sum_{i,j \in E} X_{ij}^{k_S} \leq |E_{k_S}| - 1 \\ 2 \leq |E_{k_S}| \leq N_{k_S} - 1 \end{cases}, (k_S \in C_S), \quad (17)$$

$$\begin{cases} \sum_{m,n \in P_i} X_{mn}^{k_i} \leq |E_{k_i}| - 1 \\ 2 \leq |E_{k_i}| \leq N_{k_i} - 1 \end{cases}, (k_i \in C_i). \quad (18)$$

3. An improved grey wolf optimizer

3.1. Grey wolf optimizer

The Grey Wolf Optimizer (GWO) is a novel swarm intelligence optimization algorithm introduced by Mirjalili et al. in 2014, simulating the hierarchical structure and hunting behavior of grey wolf packs [21]. It offers advantages such as strong local search capability, fast convergence speed, and minimal control parameters. In the algorithm, the grey wolf population is divided into four hierarchical levels: α -wolf, β -wolf, δ -wolf, and ω -wolf, shown in Fig. 2. The hunting process involves encircling, chasing, and attacking, with the ω -wolf's updates guided by the leadership of the first three levels.

Assuming in a D -dimensional search space, the position vector of each grey wolf individual in the pack is represented as $X = (X_1, X_2, \dots, X_D)$, the iterative formula for the wolf pack's encircling prey behavior can be expressed by Eqs. (19) and (20).

$$D = |C \cdot X_p(t) - X(t)|, \quad (19)$$

$$X(t+1) = X_p(t) - A \cdot D, \quad (20)$$

where t denotes current iteration, D is the distance between individual and prey, and X_p is the prey position vector. A and C are coefficient vectors, obtained from Eqs. (21) and (22).

$$A = 2ar_1 - a, \quad (21)$$

$$C = 2r_2, \quad (22)$$

where A is the convergence factor and linearly decreases from 2 to 0 with the number of iterations, r_1 and r_2 are random numbers between (0,1).

After the wolf pack encircles the prey, it begins to hunt under the leadership of three wolves. The iterative formula of the wolf pack hunting prey can be expressed by Eqs. (23)–(25).

$$\begin{cases} D_\alpha = |C_1 \cdot X_\alpha - X| \\ D_\beta = |C_2 \cdot X_\beta - X| \\ D_\delta = |C_3 \cdot X_\delta - X| \end{cases}, \quad (23)$$

$$\begin{cases} X_1 = X_\alpha - A_1 \cdot D_\alpha \\ X_2 = X_\beta - A_2 \cdot D_\beta \\ X_3 = X_\delta - A_3 \cdot D_\delta \end{cases}, \quad (24)$$

$$X(t+1) = \frac{X_1 + X_2 + X_3}{3}. \quad (25)$$

where $X_\alpha, X_\beta,$ and X_δ represent the current position vectors of the wolves, $D_\alpha, D_\beta,$ and $D_\delta,$ the distances between the other wolves and the three wolves, and $X(t+1)$ the updated position vector for other wolves. When $|A| > 1$, the wolves are forcedly separated from their prey, then scattered in various areas in search of a prey, to find the global optimal solution. When $|A| < 1$, the wolves attack towards their prey, by searching locally around the promising region.

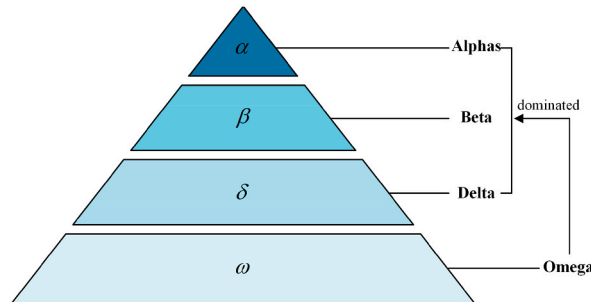


Fig. 2. Schematic diagram of the grey wolf algorithm hierarchy.

3.2. Improved grey wolf optimizer

While GWO exhibits good local optimization capability, the fact that the position updates of the wolf pack are determined by the three leader alpha, beta, and delta wolves leads to each individual converging towards the region of these leading wolves, resulting in weak global exploration ability and a susceptibility to premature convergence to local optima. Furthermore, due to the random generation of the initial population, the issue of uneven initial population distribution can arise.

This paper proposes improvements to GWO in terms of initial population and update strategy, resulting in an enhanced Grey Wolf Optimization algorithm (OLC-GWO) based on Opposition-based Learning, Levy flight strategy, and Cauchy mutation. Initially, high-quality initial wolf population is generated using Opposition-based Learning to enhance algorithm convergence. Furthermore, a hierarchical perturbation mechanism is designed, employing distinct update strategies for different rank wolves: Cauchy mutation for elite individuals (alpha, beta, and delta wolves) and Levy flight strategy for weaker individuals (omega wolf), preserving the optimal solutions. Through this mechanism, the algorithm’s global optimization capability is significantly enhanced, enabling rapid escape from local optima without compromising stability of optimal solutions.

3.2.1. Opposition-based learning

The population generated solely through random strategy lacks fitness estimation and exhibits uneven distribution, resulting in inferior solution quality and convergence speed. This paper utilizes Opposition-based Learning to enhance the population initialization strategy of GWO [22], aiming to elevate the quality of initial solutions for accelerated convergence and improved global optimization capability, as depicted in Fig. 3.

If the feasible solution in j -th dimension of the i -th grey wolf in population P is x_{ij} , the generation of the reverse population is given by Eq. (26):

$$x'_{ij} = \rho(x_{\min}^j + x_{\max}^j - x_{ij}). \tag{26}$$

where ρ is the inverse factor, while x_{\max}^j and x_{\min}^j are respectively the maximum and minimum values of feasible solutions in the j -th dimension.

Therefore, the initialization steps of opposition-based learning population are as follows:

- (1) Generate the initial population through a random strategy.
- (2) Generate an opposition population based on the initial population.
- (3) Sequentially select corresponding individuals from both populations, calculate their fitness, and utilize a greedy strategy to choose the higher fitness individual to be placed in the initial population.
- (4) Sequentially compare all individuals to obtain a higher-quality initial population for algorithm utilization.

3.2.2. Levy flight strategy

To address the issue of premature convergence in GWO, an improvement is made to the update strategy by introducing the Levy flight strategy [23]. The Levy flight refers to a random walk with a heavy-tailed distribution for step lengths. This phenomenon is common in the natural world where organisms search for food in unknown environments. It exhibits characteristics of frequent short-distance searches and occasional long-distance searches, effectively expanding the algorithm’s search range and enhancing local optimization. With the incorporation of the Levy strategy, the update formula for the ω wolf is presented in Eqs. (27)–(30).

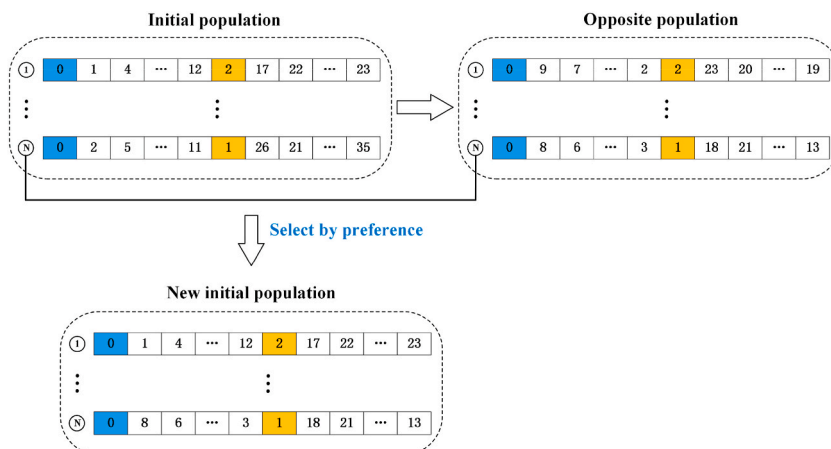


Fig. 3. Schematic diagram of population initialization based on opposition-based learning.

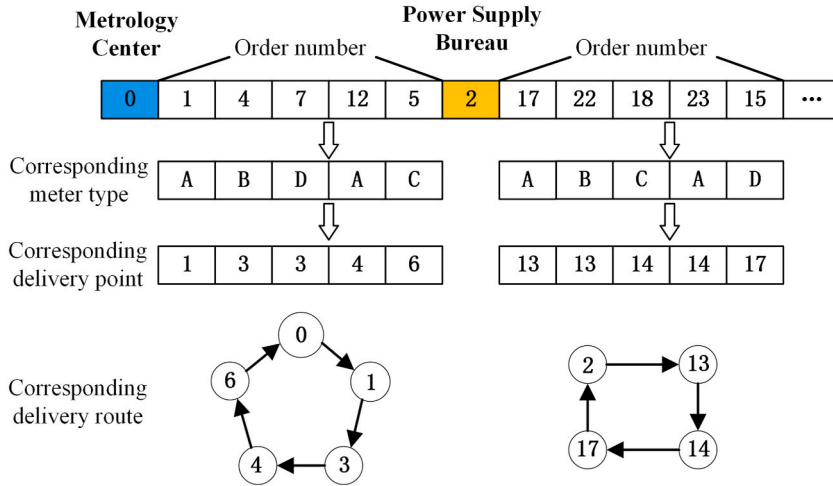


Fig. 4. Schematic diagram of individual coding of the grey wolf.

$$X(t+1)_{new} = \begin{cases} \frac{1}{3} \times (X_\alpha - A_1 \cdot D_\alpha + X_\beta - A_2 \cdot D_\beta + X_\delta - A_3 \cdot D_\delta) + \theta \oplus Levy(\beta), & |A| \geq 0.5 \\ \frac{1}{3} \times (X_\alpha - A_1 \cdot D_\alpha + X_\beta - A_2 \cdot D_\beta + X_\delta - A_3 \cdot D_\delta), & |A| < 0.5 \end{cases}, \quad (27)$$

where β is a random number between 0 and 2,

$$\theta \oplus Levy(\beta) \sim 0.01 \frac{u}{|v|^{-\beta}} (X(t) - X_a(t)), \quad (28)$$

$$u \sim N(0, \sigma_u^2), v \sim N(0, \sigma_v^2), \quad (29)$$

$$\sigma_u = \left[\frac{\Gamma(1 + \beta) \sin\left(\frac{\pi\beta}{2}\right)}{\Gamma\left(\frac{1+\beta}{2}\right) \beta \times 2^{\frac{\beta-1}{2}}}\right]^{\frac{1}{\beta}}, \sigma_v = 1, \quad (30)$$

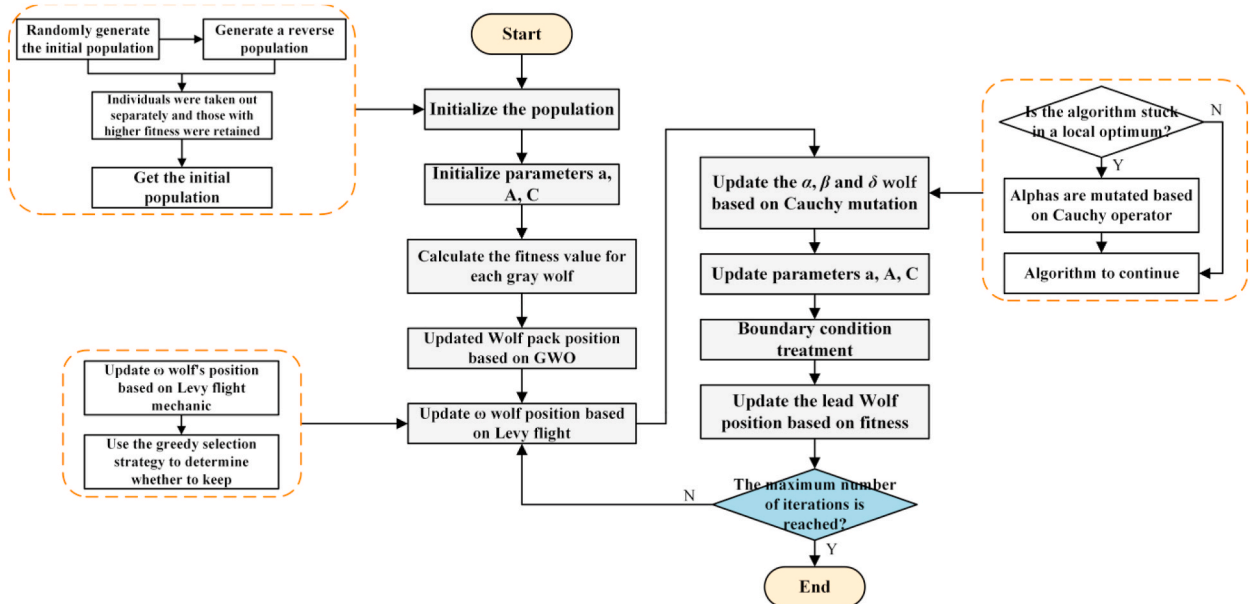


Fig. 5. General flow chart of the improved grey wolf algorithm.

In addition, the decision of whether to keep the updated individuals is then based on the greedy strategy as well as the random number r_{new} , as shown in Eq. (31).

$$X(t+1) = \begin{cases} X(t), & f(X_{new}(t)) > f(X(t)) \text{ and } r_{new} < p \\ X_{new}(t), & \text{otherwise} \end{cases} \tag{31}$$

where both r_{new} and p are random numbers between [0,1].

3.2.3. Cauchy mutation

When the alpha wolf falls into a local optimum, other individuals also tend to converge towards the alpha wolf's region, potentially preventing the algorithm from achieving the global optimal solution. To further address these issues, this paper introduces the Cauchy mutation operator based on the genetic algorithm's mutation concept to enhance population diversity [24]. This addition assists the population in swiftly escaping local optima. During the later iterations of the algorithm, specifically when the iteration count "t" reaches half of the maximum iteration count T_{max_iter} , a determination is made to identify if the algorithm is trapped in a local optimum. The mechanism for detecting whether the algorithm is trapped in a local optimum is shown in Eq. (32), where we define that if the global optimum fitness remains unchanged for five consecutive generations, the algorithm is deemed to be stuck in a local optimum.

$$\begin{cases} \text{Local optimal solution} & , \text{ if } f(X(t)) = f(X(t-1)) = \dots = f(X(t-4)) \\ \text{Continue} & , \text{ else} \end{cases} \tag{32}$$

When the determination algorithm falls into a local optimum, as shown in Eqs. (33) and (34), the three head wolves, i.e., α , β , and δ wolves, are mutated by the Cauchy operator.

$$X_\alpha(t+1) = X_\alpha(t) + X_\alpha(t) \times \text{Cauchy}(0, 1), \tag{33}$$

$$\text{Cauchy}(0, 1) = \tan((\text{rand} - 0.5) \times \pi). \tag{34}$$

Finally, the fitness of the updated individuals is compared with their previous fitness, and the superior ones are retained as individuals in the new generation of the population.

3.2.4. Algorithm coding

To ensure the algorithm's solution satisfies the numerous constraints in the established model, during the algorithm's update process, model constraint validation is based on the mapping relationship between vehicle ID, vehicle type, and orders. Throughout the distribution, all carrier orders must be fulfilled by vehicles to meet the demands of power bureaus/substations. Each vehicle's load is determined based on the orders it carries; if it violates the load limit, order-vehicle reallocation is performed. The individual's encoding and decoding process is depicted in Fig. 4. To maintain sub-routes between vehicle distribution networks and establish sub-circuits, after obtaining distribution paths based on the order-receiving point mapping, departure points are added to the distribution paths to satisfy sub-circuit constraints.

Based on this, using the obtained vehicle distribution paths, the distance of vehicle delivery paths can be calculated. If it doesn't

Table 1
Benchmarking mathematical functions.

Type of function	Functions	Dimension	Range of Functions	Theoretical minimum value
Unimodal benchmark functions	$f_1(x) = \sum_{i=1}^n x_i^2$	30	[-100,100]	0
	$f_2(x) = \sum_{i=1}^n x_i + \prod_{i=1}^n x_i $	30	[-10,10]	0
	$f_3(x) = \sum_{i=1}^{n-1} [100(x_{i+1} - x_i)^2 + (x_i - 1)^2]$	30	[-30,30]	0
	$f_4(x) = \sum_{i=1}^n ([x_i + 0.5])^2$	30	[-100,100]	0
	$f_5(x) = \sum_{i=1}^n ix_i^4 + \text{random}[0, 1]$	30	[-1.28,1.28]	0
Multimodal benchmark functions	$f_6(x) = \sum_{i=1}^n -x_i \sin(\sqrt{ x_i })$	30	[-500,500]	-418.9829*dim
	$f_7(x) = \sum_{i=1}^n [x_i^2 - 10 \cos(2\pi x_i) + 10]$	30	[-5.12,5.12]	0
	$f_8(x) = \frac{1}{4000} \sum_{i=1}^n x_i^2 - \prod_{i=1}^n \cos\left(\frac{x_i}{\sqrt{i}}\right) + 1$	30	[-600,600]	0
Fixed-dimension multimodal benchmark functions	$f_9(x) = \left[\frac{1}{500} + \sum_{j=1}^{25} \frac{1}{\sum_{i=1}^2 (x_i - a_{ij})^6} \right]^{-1}$	2	[-65.536,65.536]	1
	$f_{10}(x) = 4x_1^2 - 2.1x_1^4 + \frac{1}{3}x_1^6 + x_1x_2 - 4x_2^2 + 4x_2^4$	2	[-5,5]	-1.0316285
	$f_{11}(x) = -\sum_{i=1}^4 c_i \exp[-\sum_{j=1}^3 a_{ij}(x_j - p_{ij})^2]$	3	[1,3]	-3.86
	$f_{12}(x) = -\sum_{i=1}^5 [(x - a_i)(x - a_i)^T + c_i]^{-1}$	4	[0,10]	-10.1531

comply with the vehicle path constraint, orders are reassigned to vehicles to satisfy vehicle performance constraints. Finally, to address maximum service level and maximum storage capacity constraints, thresholds are set for metering center to power supply bureau judgment.

For the choice of algorithm termination conditions, common options in existing optimization algorithms include maximum fitness evaluation and maximum iteration count. The relationship can be expressed as the evaluation count = population size * iteration count, where the maximum fitness evaluation is suitable for situations where the population size is not fixed and changes with the increase of iteration count. For the designed OLC-GWO in this paper, high-quality initial feasible solutions are obtained through the introduction of Opposition-based Learning. However, since the population size remains constant throughout the algorithm's iteration process, the effects of the two termination conditions are equivalent. As a result, in the simulation process, this paper still uses the more commonly used maximum iteration count as the algorithm's termination condition.

3.2.5. Algorithm pseudocode

Pseudocode of the OLC-GWO	
	%%%%%%%% Initialize population and parameters %%%%%%%%%
	% Aparameters are structured parameters of the algorithm
	% Initialize the population based on the opposition-based learning strategy,
	% and calculate the individual fitness
1	X = Oppositional (Aparameters);
2	for i = 1:NP
3	orderInfo = getOrder(X(i,:));
4	pathInfo = getPath(X(i,:));
5	fit(i) = fitness(X(i,:),orderInfo(i,:),pathInfo(i,:));
6	Endfor
7	Initialize parameters a, A, C
8	Record the first three individuals with the best fitness as the head wolf
	%%%%%%%% Start iterative optimization %%%%%%%%%
9	while l < Max_iter
10	for i = 1:size(X, 1)
11	Updated wolf pack position based on GWO;
12	Update ω wolf location based on Levy flight mechanic;
14	Update α, β and δ wolf location based on Cauchy mutation;
15	Update parameters a, A, C;
16	Calculate individual fitness and update the head wolf;
17	endif
18	for j = 1:D
19	Boundary condition treatment;
20	endifor
21	orderInfo = getOrder(x(i,:));
22	pathInfo = getPath(x(i,:));
23	fit(i) = fitness(X(i,:),orderInfo(i,:),pathInfo(i,:));
24	endifor
	%%%%%%%% Algorithm ends %%%%%%%%%
25	Output

3.2.6. Algorithm flowchart

The overall flow chart of the algorithm is shown in Fig. 5.

4. Benchmark function test

In this paper, MATLAB R2022a is utilized as a programming tool for function testing of the algorithm as well as simulation solution of the model. The simulations were run on a computer with Win11 operating system, 16 GB RAM, AMD Ryzen 7 5800U CPU and NVIDIA GeForce RTX 3050 Laptop GPU. To demonstrate the superior optimization capability of the designed OLC-GWO compared to other state-of-the-art optimization algorithms, it is compared against traditional GWO, PSO, Harris Hawk Optimization (HHO), Honey Bee Algorithm (HBA), and Multi-Verse Optimizer (MVO) through benchmark function testing and simulation experiments.

Furthermore, in other relevant literature, various variants and improvements of GWO can be observed. In this study, we compare our algorithm with the advanced Grey Wolf Optimization Algorithm (AGWO) proposed by Ahmadi et al. [19] to demonstrate the effectiveness and practical value of the modifications made to GWO in this paper.

The parameters of each comparison algorithm are set as follows: in OLC-GWO the reverse learning factor $\rho = 1$; in AGWO the parameters are the same as in the original paper; in PSO the learning factor $c1 = c2 = 1.5$, the upper speed limit $Vmax = 10$ and the lower limit $Vmin = -10$; in HBA the ability to get food $beta = 6$ and the constant $C = 2$; in MVO the upper and lower bounds on the WEP probability of the existence of wormholes are 1 and 0.2, respectively.

The selected Benchmarking mathematical functions for testing are as presented in Table 1. These include Unimodal benchmark

functions, Multimodal benchmark functions, and Fixed-dimension multimodal benchmark functions, each depicted graphically in Fig. 6. To ensure a more illustrative comparison of results due to varying search difficulty and convergence speed among different functions, this experiment employs diverse settings for the maximum iteration count T_{\max_iter} for each test function. Ensuring fairness, all algorithms run with equal maximum iteration counts on the same function, with a population size N of 100. Each algorithm is independently executed 10 times on each test function set, and their average iteration curves are demonstrated in Fig. 7, while their average performance metrics are summarized in Table 2.

From a qualitative perspective, as observed from the average iteration curves in Fig. 7, OLC-GWO demonstrates a faster convergence rate. It exhibits strong convergence capability both in the early and later stages of iteration. The optimal fitness of the population decreases with an increase in iteration count, and the oscillation amplitude inversely diminishes as iterations progress. In other words,

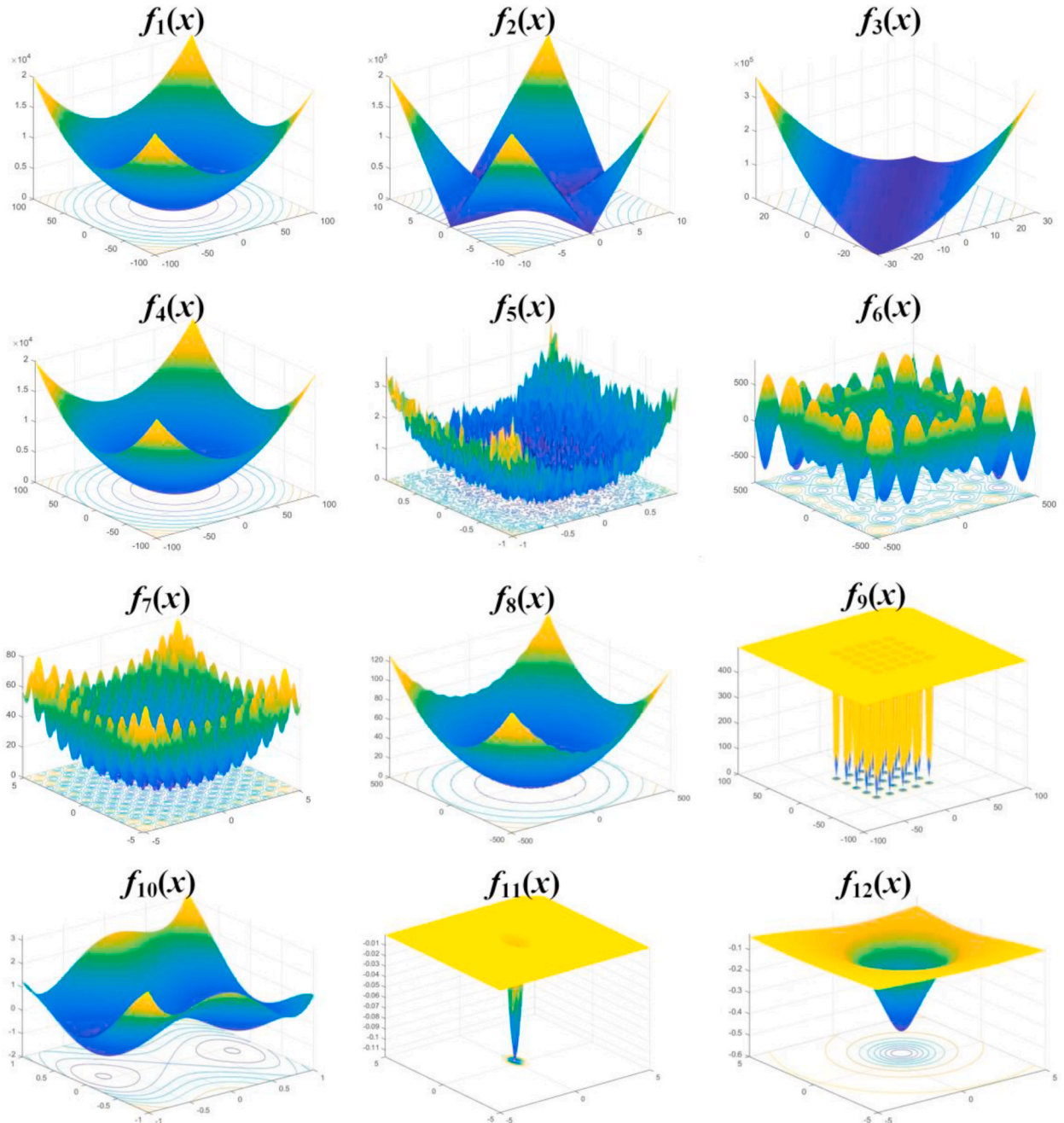


Fig. 6. The function image of each benchmark test function used. ($f_1(x) - f_{12}(x)$ in the graph correspond to each function in Table 1, respectively.).

throughout the optimization process, the algorithm transitions from a broad global search to a more refined local search, leading to a gradual flattening of the curve.

From a quantitative analysis perspective, as evident from the 12 sets of test results in Table 2, the algorithm designed in this study

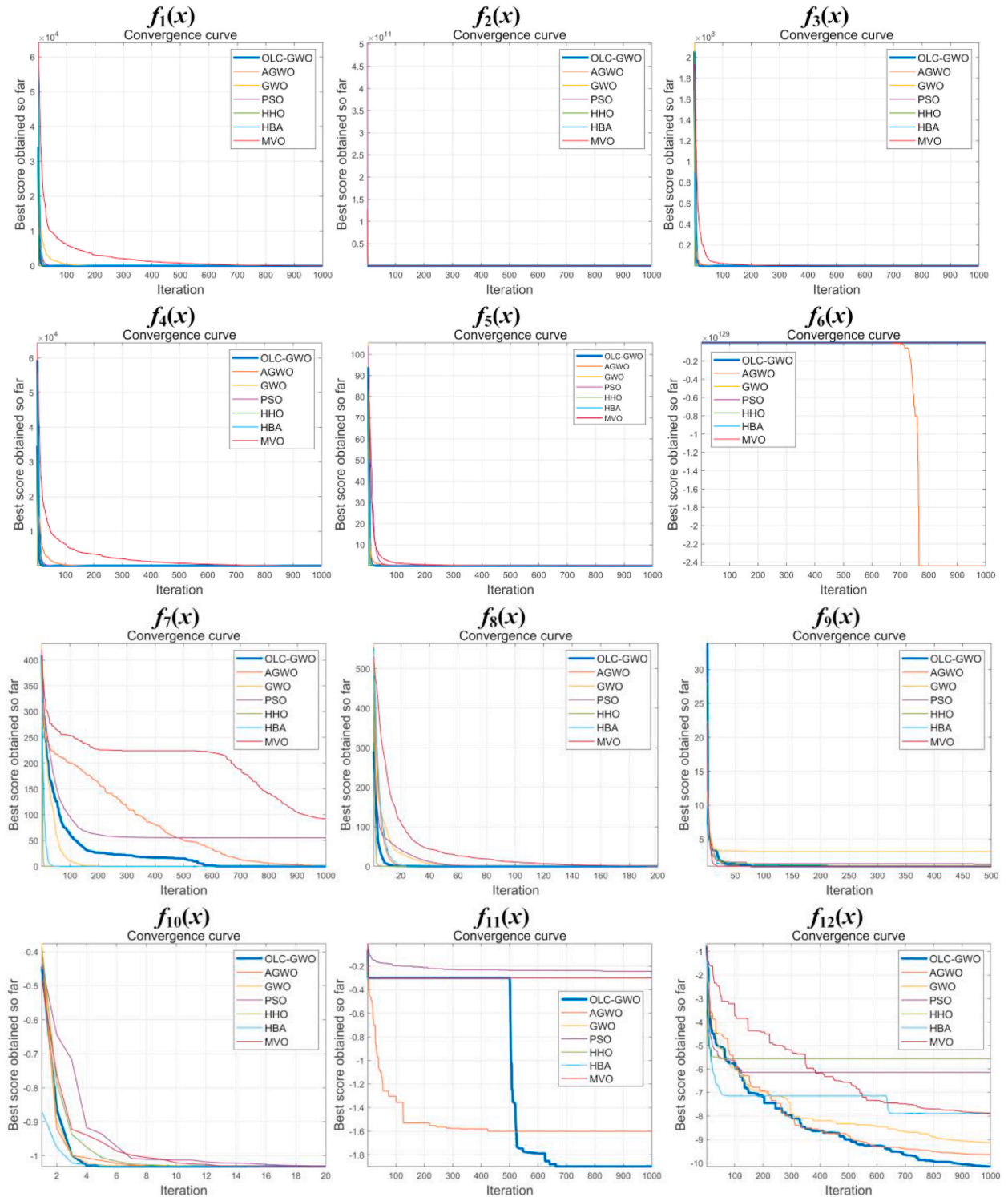


Fig. 7. Average iteration curve of OLC-GWO on each test function. ($f_1(x) - f_{12}(x)$ in the graph correspond to each function in Table 1, respectively.).

Table 2
Average objective function value for each algorithm.

Function	$f_1(x)$	$f_2(x)$	$f_3(x)$	$f_4(x)$	$f_5(x)$	$f_6(x)$
T_{iter}	1000	1000	1000	1000	1000	1000
OLC-GWO	0	1.5031e-172	1.9567e-07	2.6677e-12	1.475e-05	-6.74046e+30
AGWO	8.6325e-86	1.0249e-106	0.015719	6.0534e-06	0.00024356	-2.44080 + 129
GWO	2.9832e-11	3.4035e-49	0.20215	0.10049	0.0026012	-5988.2667
PSO	1.6569	7.1542	954.2735	1.868	0.1443	-7347.4405
HHO	2.5832e-207	5.4707e-07	0.11274	1.1148e-06	0.0031096	-12569.4767
HBA	1.4314e-67	2.3810e-33	18.5178	0.0056124	5.8801e-05	-10048.429
MVO	0.09203	0.21264	109.6747	0.099237	0.0058303	-7768.8798
Function	$f_7(x)$	$f_8(x)$	$f_9(x)$	$f_{10}(x)$	$f_{11}(x)$	$f_{12}(x)$
T_{iter}	1000	200	500	20	1000	1000
OLC-GWO	0	0	0.998	-1.0316	-1.89950	-10.1530
AGWO	0	0.0023481	0.998	-1.0316	-1.60040	-9.6433
GWO	0	0.051423	3.165	-1.0316	-0.30048	-9.1381
PSO	55.2827	0.29596	1.2958	-1.0297	-0.24445	-6.1448
HHO	0	0	1.0974	-1.0316	-0.30048	-5.5650
HBA	0	0.011803	0.998	-1.0316	-0.30048	-7.8964
MVO	92.1794	1.0054	0.998	-1.0315	-0.30048	-7.8806

consistently achieves the best performance across most test functions. This demonstrates that OLC-GWO excels in various optimization problems. Particularly, when solving Fixed-dimension multimodal benchmark functions, OLC-GWO displays enhanced competitiveness compared to other similar algorithms, indicating its greater advantage in solving the large-scale scheduling model proposed in this paper.

5. Simulation analysis

This paper conducts a case study on the centralized distribution of electricity meters by a provincial metrology center. An optimal scheduling scheme for meter rotation and distribution is solved using a sample of electricity meter orders from a specific time period. Initially, each power substation reports the electricity meter demands to their respective power supply bureau on schedule. These power supply bureaus then consolidate their needs along with the demands of their subordinate substations and report to the metering center. Finally, the metering center conducts unified distribution. The distance matrix for the provincial metering center-power supply bureau-power substation is presented in Table 3. The hierarchical relationship between power supply bureaus and power substations is illustrated in Fig. 8. The demand for orders from power supply bureaus to substations is shown in Table 4.

The types of electricity meters and related parameters are shown in Table 5, and the parameters of outsourced vehicles are shown in Table 6.

The parameters of each algorithm are set as above. Set the model parameters as follows: labor distribution cost to reach a single site $C_p = 20(\text{CNY})$, labor cost per unit time of a vehicle transport $G = 50(\text{CNY})$.

Each algorithm was executed 50 times. The comparative evolution iteration curves of average fitness for each algorithm across different hierarchical distribution networks are shown in Figs. 9–12. The obtained optimized scheduling schemes are presented in Table 7. The average fitness values for each hierarchical distribution network are provided in Table 8.

As observed from Figs. 9–12, after incorporating improvements like Opposition-based Learning and Levy flight, OLC-GWO

Table 3
Distance matrix for each node.

Position two	Position one					
	Yunnan Power Grid Corporation Metering Center	Yunnan Power Grid Dali Power Supply Bureau	...	Jianchuan Power Supply Bureau	...	Shuifu City Power Supply Bureau
China Southern Power Grid Qujing Power Supply Bureau	142	447	...	480	...	514
Yunnan Power Grid Corporation Kylin Power Supply Bureau	153	457	...	489	...	516
...
China Southern Power Grid Xuanwei Power Supply Branch	236	544	...	576	...	422
Zhaotong Power Supply Bureau	346	655	...	689	...	220
...
Zhaotong Ludian County Power Supply Bureau	331	640	...	672	...	252
Yanjin County Power Supply Company	487	795	...	828	...	116

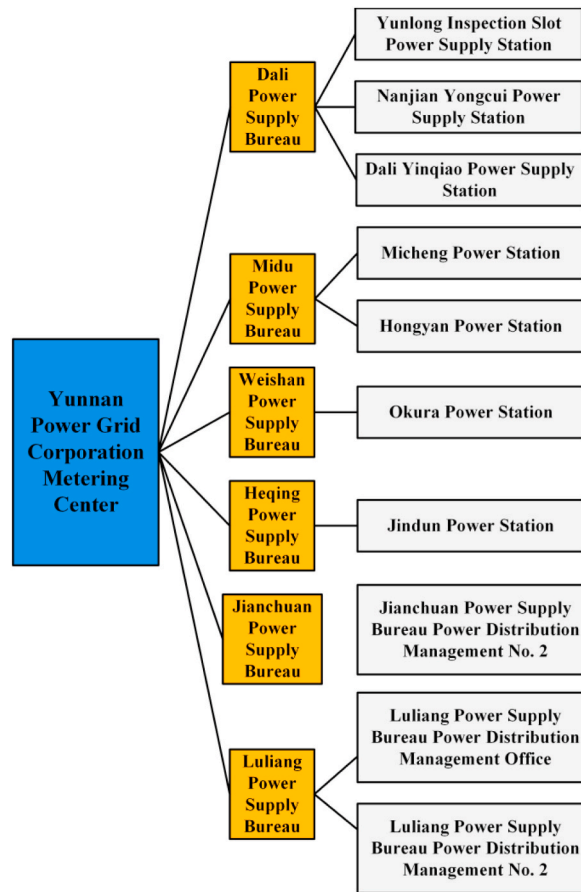


Fig. 8. The affiliations of metering center - power supply bureau -power supply substation in the simulation experiment.

Table 4
Demand orders from power supply bureaus/substations.

Metrology Center		Dali Power Supply Bureau		Midu Power Supply Bureau		...	Luliang Power Supply Bureau	
type	quantity	type	quantity	type	quantity	...	type	quantity
...
3	50	1	44	1	50	...	3	38
3	50	2	50	1	44	...	4	40
3	39	2	46	2	50	...	4	40
4	40	3	50	2	46	...	4	14
4	40	3	38	3	50	...	1	50
4	40	4	40	3	38	...	1	41
4	23	4	40	4	40	...	2	50
1	43	4	14	4	40	...	2	31
2	39	1	50	4	14	...	3	50
3	34	1	41	1	50	...	3	30
4	37	2	50	1	41	...	4	40
1	32	2	31	2	50	...	4	40
2	43	3	50	2	31	...	4	13
3	37	3	30	3	50	...	1	50
4	32	4	40	3	30	...	1	48
...

demonstrates superior optimization capability and convergence speed compared to traditional GWO and similar optimization algorithms. It maintains excellent convergence performance throughout the entire search process. As evident from Table 8, in the first-tier distribution from the central measurement center, OLC-GWO’s average fitness value is reduced by 15.36%, 12.72%, 14.70%, 17.74%, and 17.93% compared to GWO, PSO, HHO, HBA, and MVO, respectively. In the second-tier distribution to substations, it is reduced by 11.32%, 7.88%, 10.03%, 7.75%, and 24.43%. This indicates the superior solution quality of the proposed algorithm over the

Table 5
Types and specifications of smart meters.

M_p	Type	Turnover box specifications β_1	Dimensions ($L \times W \times H$)	Weight	Turnover Pallet Specifications β_2
M_1	Single-phase energy meter	12/box	720 × 450 × 120(mm)	18 kg/box	5 boxes/stack
M_2	Three-phase energy meter	4/box			
M_3	Metering automation terminal	4/box			
M_4	Low voltage transformer	12/box	720 × 450 × 200(mm)	45 kg/box	2 boxes/stack

Table 6
Outsourced vehicle information parameter table.

Vehicle model	Volume (m^3)	Load limit (t)	The average daily mileage of the vehicle (km)	Quantity	Price per kilometer [CNY/(Ton • km)]
1	15	2	725	55	0.25
2	15	4	668	50	0.28
3	25	5	648	55	0.30

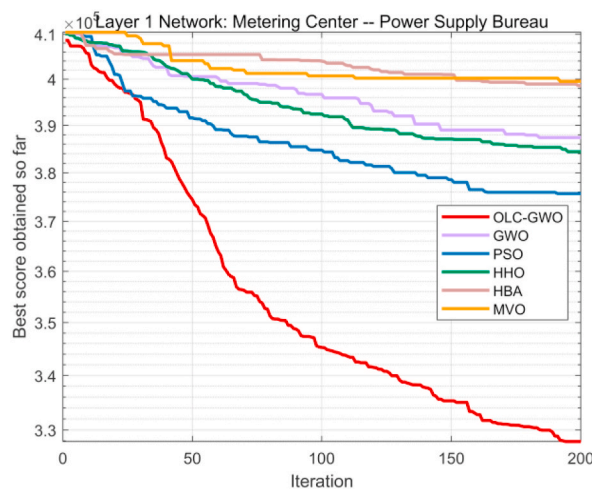
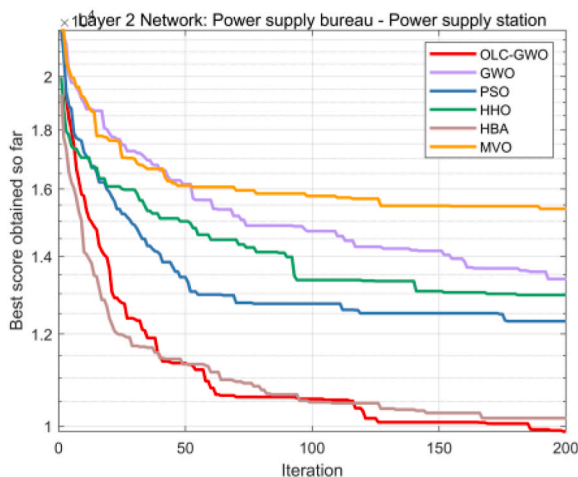
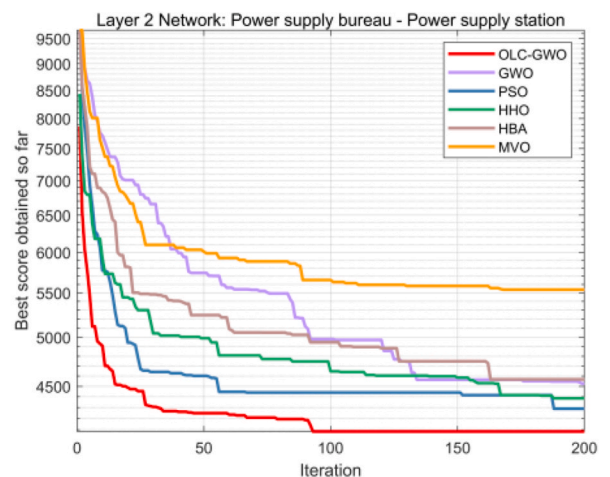


Fig. 9. The evolution curve of each algorithm in the first-level distribution network.



(a)



(b)

Fig. 10. The evolution curve of each algorithm in the distribution network of each power supply bureau at the second level. (a: Power supply bureau 1; b: Power supply bureau 2).

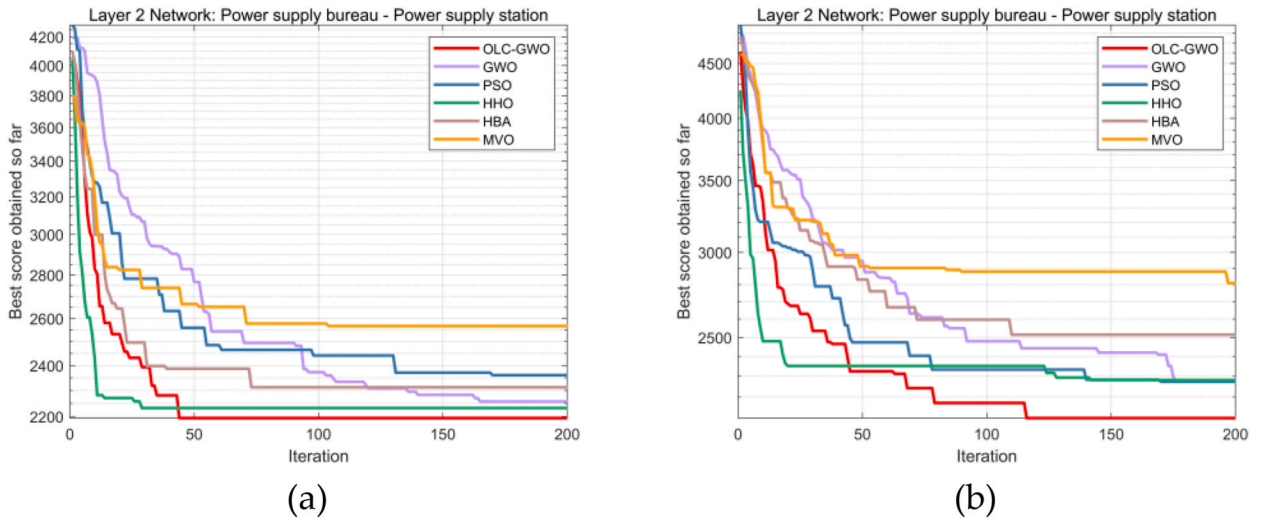


Fig. 11. The evolution curve of each algorithm in the distribution network of each power supply bureau at the second level. (a: Power supply bureau 3; b: Power supply bureau 4).

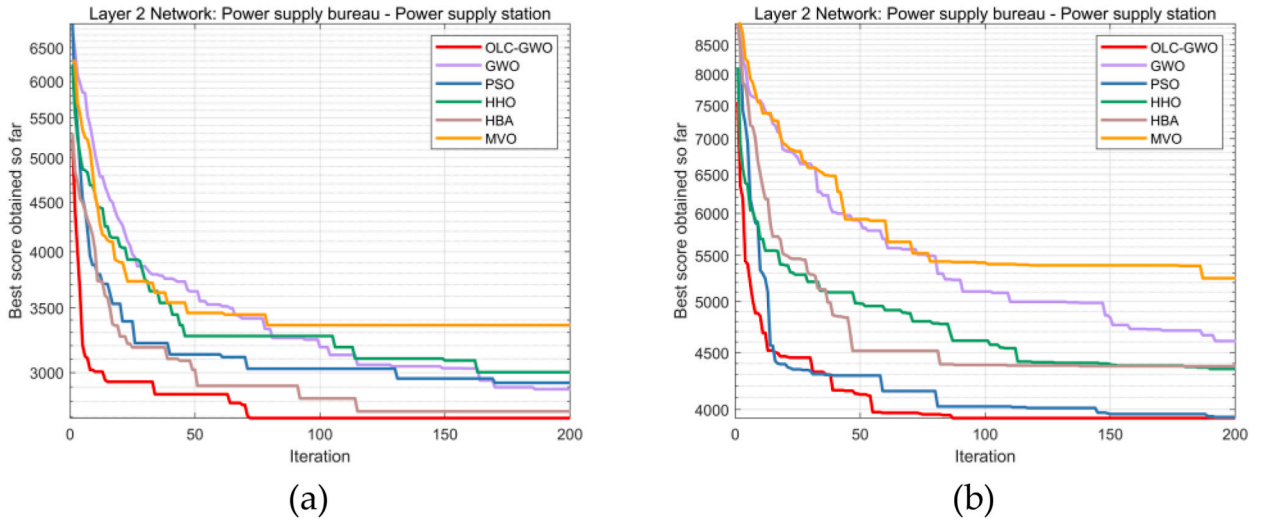


Fig. 12. The evolution curve of each algorithm in the distribution network of each power supply bureau at the second level. (a: Power supply bureau 5; b: Power supply bureau 6).

comparative methods, highlighting its strong applicability to solving large-scale logistics scheduling optimization problems.

In summary, the improved algorithm proposed in this paper outperforms other algorithms in terms of optimization capability and convergence speed. It maintains superior fitness values and convergence ability throughout the search process in various levels of scheduling networks, thanks to the Opposition-based Learning mechanism. This mechanism enhances the even distribution of individuals in the initial population, effectively improving the algorithm’s solving efficiency. Meanwhile, the Levy flight mechanism and Cauchy mutation mechanism enable OLC-GWO to swiftly escape local optima without losing the optimal solution, enhancing the algorithm’s precision in solving.

6. Conclusions

This paper investigates the vehicle scheduling problem for large-scale smart meter rotation, addressing vehicle cost, time cost, and transportation distribution cost by establishing a multi-level optimization model for distribution vehicle scheduling. An improved Grey Wolf algorithm is proposed using Opposition-based Learning, Levy flight strategy, and Cauchy mutation for solution. Opposition-based Learning enhances population diversity and obtains high-quality initial feasible solutions. The incorporation of Levy flight strategy and Cauchy mutation broadens the algorithm’s optimization scope and global optimization capability. Feasibility is verified through early-

Table 7
Vehicle scheduling results at all levels.

Order	The specific route	Transport models
First level distribution		
1	Metering Center—Xiangyun Power Supply Bureau-Heqing Power Supply Bureau-Yangbi Power Supply Bureau-Measuring Center	1
2	Metering Center-Dali Power Supply Bureau-Yangbi Power Supply Bureau-Jianchuan Power Supply Bureau-Heqing Power Supply Bureau-Measuring Center	1
3	Metering Center-Dali Power Supply Bureau-Weishan Power Supply Bureau-Maidu Power Supply Bureau-Yunlong Power Supply Bureau-Metering Center	1
4	Metering Center-Yongping Power Supply Bureau-Qujing Power Supply Bureau-Qujing Luoping Power Supply Bureau-Metering Center	2
5	Metering Center-Weishan Power Supply Bureau-Xiangyun Power Supply Bureau-Nanjian Power Supply Bureau-Measuring Center	2
6	Measurement Center-Qujing Power Supply Bureau-Qilin Power Supply Bureau-Weishan Power Supply Bureau-Malong Power Supply Bureau-Measurement Center	3
7	Metering Center-Jianchuan Power Supply Bureau-Weishan Power Supply Bureau-Xiangyun Power Supply Bureau-Metering Center	3
...
Second level distribution		
1	Dali Power Supply Bureau-Dali Yinqiao Power Supply Office-Maidu Yicheng Power Supply Office-Dali Power Supply Bureau	1
2	Weishan Power Supply Bureau-Weishan Dacang Power Supply Office-Nanjian Power Supply Bureau-Weishan Power Supply Bureau	1
3	Luliang Power Supply Bureau - Luliang Power Supply Bureau Distribution Management No.2 - Luliang Power Supply Bureau Distribution Management Office - Luliang Power Supply Bureau	2
4	Jianchuan Power Supply Bureau-Jianchuan Power Supply Bureau Distribution Management No.2-Jianchuan Power Supply Bureau	2
5	Heqing Power Supply Bureau - Heqing Jindun Power Supply Office - Heqing Power Supply Bureau	3
...

Table 8
Fitness comparison of each algorithm.

Index	Algorithm					
	OLC-GWO	GWO	PSO	HHO	HBA	MVO
The first-layer distribution network: the average objective function value of the metering center-power supply bureau						
Average fitness (10^5)	3.2790	3.8742	3.7568	3.8442	3.9859	3.9954
The second-layer distribution network: the average objective function value of each power supply bureau- power substation						
Average fitness I (10^4)	0.9894	1.3386	1.2310	1.2967	1.0159	1.5385
Average fitness II (10^3)	4.0834	4.5274	4.2889	4.3858	4.5682	5.5379
Average fitness III (10^3)	2.1940	2.2574	2.3610	2.2324	2.3126	2.5667
Average fitness IV (10^3)	2.1024	2.2816	2.2735	2.2816	2.5145	2.8090
Average fitness V (10^3)	2.6920	2.8832	2.9277	3.0029	2.7355	3.3590
Average fitness VI (10^3)	3.9302	4.6089	3.9385	4.3506	4.3754	5.2479

stage work using Benchmarking mathematical functions, and simulation experiments compare it with other state-of-the-art swarm intelligence algorithms, demonstrating the feasibility and practicality of the proposed model and algorithm in the field of smart grid logistics scheduling. In conclusion, the main contributions of this paper are as follows:

- Constructs a multi-level distribution network scheduling model for large-scale smart meter batch rotation scenarios, accounting for multidimensional constraints in real-world meter distribution contexts, providing practicality and generalizability.
- Introduces an improved Grey Wolf algorithm for solving the model, exhibiting greater competitiveness compared to similar algorithms.
- Employs simulation parameters and data derived from actual distribution business data in engineering projects, ensuring the experiment’s authenticity and the practicality of the solution results.

The conclusions drawn from our study, although noteworthy, do come with certain limitations. It is acknowledged that the model we have developed may not comprehensively encompass the multidimensional constraints that arise in real-world distribution scenarios. Additionally, it might struggle to dynamically adapt to the uncertainties encountered during the actual scheduling processes. Despite these constraints, the significance and potential for broader application of our work in the realm of logistics and scheduling cannot be ignored. Our study offers valuable insights and serves as a solid foundation for future research endeavors in this domain.

In subsequent investigations, there is room for enhancing and expanding the model’s structure to augment its practical applicability in real-world scenarios. Moreover, the model’s generalizability could be extended to encompass a wider array of practical engineering projects across various domains. By addressing these limitations and pursuing these avenues for improvement, our work’s practical value can be further elevated.

Funding

This work was supported in part by the Science and technology project of China Southern Power Grid Co., Ltd. (YNKJXM20220174, YNKJXM20220010).

Code availability statement

The source code of the benchmark function test section and the generated dataset are available from the corresponding author upon reasonable request.

CRedit authorship contribution statement

Zhaolei He: Conceptualization, Methodology, Software, Writing – original draft, Funding acquisition. **Xinbo Zhou:** Conceptualization, Methodology, Software, Validation, Visualization, Writing – original draft, Writing – review & editing. **Cong Lin:** Data curation, Methodology, Resources, Software. **Jing Zhao:** Data curation, Formal analysis, Methodology. **Hengjie Yu:** Data curation, Resources. **Rui Fang:** Conceptualization, Data curation. **Jin Liu:** Data curation, Investigation, Supervision. **Xin Shen:** Data curation, Supervision. **Nan Pan:** Conceptualization, Formal analysis, Funding acquisition, Methodology, Supervision.

Declaration of competing interest

The authors declare that they have no known competing financial interests or personal relationships that could have appeared to influence the work reported in this paper.

References

- [1] N.P.G. Bhavani, Ravi Kumar, Bhawani Sankar Panigrahi, Kishore Balasubramanian, B. Arunsundar, Zulkiflee Abdul-Samad, Abha Singh, Design and implementation of IoT integrated monitoring and control system of renewable energy in smart grid for sustainable computing network, *Sustain. Comput. Inform. Syst.* 35 (2022) 100769, <https://doi.org/10.1016/j.suscom.2022.100769>.
- [2] R.J. Kuo, Muhammad Fernanda Luthfiansyah, Nur Aini Masruroh, Ferani Eva Zulvia, Application of improved multi-objective particle swarm optimization algorithm to solve disruption for the two-stage vehicle routing problem with time windows, *Expert Syst. Appl.* 225 (2023) 120009, <https://doi.org/10.1016/j.eswa.2023.120009>.
- [3] Reza Moghdani, Khodakaram Salimifard, Emrah Demir, Abdelkader Benyettou, The green vehicle routing problem: a systematic literature review, *J. Clean. Prod.* 279 (2021) 123691, <https://doi.org/10.1016/j.jclepro.2020.123691>.
- [4] Erdi Dasdemir, Murat Caner Testik, Diclehan Tezcaner Öztürk, Ceren Tuncer Şakar, Güldal Güleriyüz, Özlem Müge Testik, A multi-objective open vehicle routing problem with overbooking: exact and heuristic solution approaches for an employee transportation problem, *Omega* 108 (2022) 102587, <https://doi.org/10.1016/j.omega.2021.102587>.
- [5] Huizhen Zhang, Qinwan Zhang, Ma Liang, Ziyang Zhang, Yun Liu, A hybrid ant colony optimization algorithm for a multi-objective vehicle routing problem with flexible time windows, *Inf. Sci.* 490 (2019) 166–190, <https://doi.org/10.1016/j.ins.2019.03.070>.
- [6] Vincent F. Yu, Panca Jodiawan, Albert H. Schrottenboer, Ming-Lu Hou, The two-echelon vehicle routing problem with time windows, intermediate facilities, and occasional drivers, *Expert Syst. Appl.* 234 (2023) 120945, <https://doi.org/10.1016/j.eswa.2023.120945>.
- [7] Thau Soon Khoo, Babrdel Bonab Mohammad, The parallelization of a two-phase distributed hybrid ruin-and-recreate genetic algorithm for solving multi-objective vehicle routing problem with time windows, *Expert Syst. Appl.* 168 (2021) 114408, <https://doi.org/10.1016/j.eswa.2020.114408>.
- [8] Yunyun Niu, Jie Shao, Jianhua Xiao, Song Wen, Zhiguang Cao, Multi-objective evolutionary algorithm based on RBF network for solving the stochastic vehicle routing problem, *Inf. Sci.* 609 (2022) 387–410, <https://doi.org/10.1016/j.ins.2022.07.087>.
- [9] Alexandra Anderluh, Pamela C. Nolz, Vera C. Hemmelmayr, Teodor Gabriel Crainic, Multi-objective optimization of a two-echelon vehicle routing problem with vehicle synchronization and 'grey zone' customers arising in urban logistics, *Eur. J. Oper. Res.* 289 (3) (2021) 940–958, <https://doi.org/10.1016/j.ejor.2019.07.049>.
- [10] Li Zhang, Zhongshan Liu, Wenxuan Shan, Bin Yu, A stabilized branch-and-price-and-cut algorithm for the waste transportation problem with split transportation, *Comput. Ind. Eng.* 178 (2023) 109143, <https://doi.org/10.1016/j.cie.2023.109143>.
- [11] Yongbo Li, Hamed Soleimani, Mostafa Zohal, An improved ant colony optimization algorithm for the multi-depot green vehicle routing problem with multiple objectives, *J. Clean. Prod.* 227 (2019) 1161–1172, <https://doi.org/10.1016/j.jclepro.2019.03.185>.
- [12] Jianyu Long, Zhenzhong Sun, Panos M. Pardalos, Ying Hong, Shaohui Zhang, Chuan Li, A hybrid multi-objective genetic local search algorithm for the prize-collecting vehicle routing problem, *Inf. Sci.* 478 (2019) 40–61, <https://doi.org/10.1016/j.ins.2018.11.006>.
- [13] Seyed Farid Ghannadpour, Fatemeh Zandiyeh, An adapted multi-objective genetic algorithm for solving the cash in transit vehicle routing problem with vulnerability estimation for risk quantification, *Eng. Appl. Artif. Intell.* 96 (2020) 103964, <https://doi.org/10.1016/j.engappai.2020.103964>.
- [14] Levi R. Abreu, Roberto F. Tavares-Neto, Marcelo S. Nagano, A new efficient biased random key genetic algorithm for open shop scheduling with routing by capacitated single vehicle and makespan minimization, *Eng. Appl. Artif. Intell.* 104 (2021) 104373, <https://doi.org/10.1016/j.engappai.2021.104373>.
- [15] M. Amine Masmoudi, Simona Mancini, Roberto Baldacci, Yong-Hong Kuo, Vehicle routing problems with drones equipped with multi-package payload compartments, *Transport. Res. E Logist. Transport. Rev.* 164 (2022) 102757, <https://doi.org/10.1016/j.tre.2022.102757>.
- [16] Junayed Pasha, Arriana L. Nwodu, Amir M. Fathollahi-Fard, Guangdong Tian, Zhiwu Li, Hui Wang, Maxim A. Dulebenets, Exact and metaheuristic algorithms for the vehicle routing problem with a factory-in-a-box in multi-objective settings, *Adv. Eng. Inf.* 52 (2022) 101623, <https://doi.org/10.1016/j.aei.2022.101623>.
- [17] Xizheng Zhang, Zeyu Wang, Zhangyu Lu, Multi-objective load dispatch for microgrid with electric vehicles using modified gravitational search and particle swarm optimization algorithm, *Appl. Energy* 306 (2022) 118018, <https://doi.org/10.1016/j.apenergy.2021.118018>. Part A.
- [18] Anees Abu-Monshar, Ammar Al-Bazi, A multi-objective centralised agent-based optimisation approach for vehicle routing problem with unique vehicles, *Appl. Soft Comput.* 125 (2022) 109187, <https://doi.org/10.1016/j.asoc.2022.109187>.
- [19] B. Ahmadi, S. Younesi, O. Ceylan, et al., An advanced grey wolf optimization algorithm and its application to planning problem in smart grids, *Soft Comput.* 26 (2022) 3789–3808, <https://doi.org/10.1007/s00500-022-06767-9>.
- [20] Xinyu Liu, Guanguan Li, Haoyuan Yang, Nianru Zhang, Longfei Wang, Shao Peng, Agricultural UAV trajectory planning by incorporating multi-mechanism improved grey wolf optimization algorithm, *Expert Syst. Appl.* 233 (2023) 120946, <https://doi.org/10.1016/j.eswa.2023.120946>.
- [21] Seyedali Mirjalili, Seyed Mohammad Mirjalili, Andrew Lewis, Grey wolf optimizer, *Adv. Eng. Softw.* 69 (2014) 46–61, <https://doi.org/10.1016/j.advengsoft.2013.12.007>.

- [22] Sarada Mohapatra, Prabhujit Mohapatra, Fast random opposition-based learning golden jackal optimization algorithm, *Knowl. Base Syst.* 275 (2023) 110679. <http://gfbfh81f8000da3924570s9v9vcufupcbf6np5.fgac.kust.cwkeji.cn/10.1016/j.knosys.2023.110679>.
- [23] S. Syama, J. Ramprabhakar, R. Anand, Josep M. Guerrero, A hybrid extreme learning machine model with Lévy flight chaotic whale optimization algorithm for wind speed forecasting, *Resul. Eng.* 19 (2023) 101274. <http://gfbfh81f8000da3924570s9v9vcufupcbf6np5.fgac.kust.cwkeji.cn/10.1016/j.rineng.2023.101274>.
- [24] Arunita Das, Amrita Namtirtha, Animesh Dutta, Lévy–Cauchy arithmetic optimization algorithm combined with rough K-means for image segmentation, *Appl. Soft Comput.* 140 (2023) 110268. <http://gfbfh81f8000da3924570s9v9vcufupcbf6np5.fgac.kust.cwkeji.cn/10.1016/j.asoc.2023.110268>.